Simple and energy efficient image compression for pulse-based communication in THz band

Muhammad Agus Zainuddin, Eugen Dedu, Julien Bourgeois
Univ. Bourgogne Franche-Comté / FEMTO-ST Institute/CNRS
Numérica, Cours Leprince-Ringuet, BP 21126, 25 201 Montbéliard, France
E-mail: {FirstName.LastName}@femto-st.fr

***Abstract*—Terahertz band (0.1–10 THz) provides very large bandwidth, enabling multimedia transmission at short distance. In macro world, ultra broadband communication networks at THz band (TeraNets) provides very large bandwidth for wireless multimedia sensor networks (WMSN). Similarly, recent development in nano-technology (nano-antenna and nano-transceiver) shows that electromagnetic nanocommunications at THz band support very large bandwidth too, which enables the development of wireless multimedia nano-sensor networks (WMNSN). For both WMSN and WMNSN, the major challenges are simple and energy efficient transmission, since the network consists of a large number of nodes with limited battery capacity. In this paper, we propose a simple, energy efficient and robustness-aware image compression for pulse-based WMSN and WMNSN. We investigate the system performance in terms of image quality, energy efficiency, perpetual operation in nanocommunications and transmission robustness against error. The results show that for these networks, with the trade-off of image quality, the proposed method outperforms JPEG, JPEG 2000, GIF and PNG in all used metrics, for example the energy reduction compared to uncompressed is 77% for JPEG and 90% for our method.**

I. Introduction

The integration of low-power wireless networking technology and multimedia microelectronics fosters the development of wireless multimedia sensor networks (WMSN) [1]. A node in WMSN has sensing, processing and communication capability to send the information to an end system. In macro scale, WMSN have applications as varied as artificial retina, battlefield surveillance, movement monitoring, volcano monitoring, tsunami or early flood detection [2]. While in micro scale, wireless multimedia nano-sensor networks (WMNSN) allow nano-devices to detect the presence of virus, harmful bacteria and cancer cell in human body [3].

Whether in macro or micro, a node in WMSN has limited resources in transmission range and energy capacity. The main research challenge in WMSN is obtaining energy efficiency to prolong the node lifetime, due to limited battery capacity and difficult process to replace or recharge the battery. Thus, it is essential to reduce the energy consumption whether in computation or in communications process.

In macro scale, wireless sensor networks, energy consumption for transmission (of 1 bit) is considerably larger than computation (execution of 1 instruction) [4], [2], [5], [6]. In [4], the authors described that the energy cost to execute 3 million instructions is 3 J, so the computation consumes 1 μJ/instruction. More recent results show that in computation, conventional microprocessor consumes 1 nJ/instruction, low-energy digital signal processing (DSP) consumes 0.01 nJ/instruction and hardwired logic consumes 0.001 nJ/instruction [5].

As for transmission in macro scale, in [4], the transmission of a 1 kbit packet over a distance of 1 km using BPSK modulation consumes energy 3 J, which is the same as executing 3 million instructions. Hence, the ratio between transmission and computation is 1:3000. In Ultra-Wide Band (UWB) image transmission system using On-Off Keying (OOK) modulation, radio transmission component consumes $P = 15$ mW with rate $R = 1.3$ Mbps for distance of 4 m [7]. So, the energy consumption is $E = P/R = 11.5$ nJ/pulse, which is three orders of magnitude more than required energy to execute 1 instruction in low-energy DSP.

In micro scale (nanonetworks), computation energy in nano-devices remains unknown, since nano-processor using graphene-based nano-transistor is under development [8]. The pulse energy in nanocommunications depends on the targeted distance between transmitter and receiver. State of the art in nanocommunications shows that pulse energy 1 pJ [9] enables transmission up to several meters, while 1 aJ [10] for several millimeters (detail in Sec. III-B). The initial prediction for computation energy in nano-devices has been reported in [11], which is 0.1 aJ per instruction. So, in micro scale too, the transmission energy is larger than computation energy.

The previous numbers consider only the transceiver part. However energy consumption for transmission also include the process where central processing unit (CPU) reads the bitstream in memory and gives instructions to signal generator for transmission process, so this process further increases the transmission energy. Moreover, for large transmission distance (e.g. more than 100 meters), transmitter requires power amplifier which consumes much energy. Since nodes in WSN have short transmission range due to the use of low power transmitter, end-to-end transmission is performed in multi-hop fashion. Therefore, total energy consumption for transmission is equal to the sum of transmission energy in each hop from source node to end system. So the transmission energy is even greater. Based on all this information, we conclude that

This work has been funded by the Ministry of Education and Culture, Indonesia (Ph.D. grant no. 435/E4.4/K/2013), and by Pays de Montbeliard Agglomeration.

computation consumes much less energy than communication. These results motivate the use of compression method before transmission process.

Now we turn our focus on the networks where the compression method can be implemented. Our particular pulse-based communication networks are TeraNets (ultra-broadband communication networks at terahertz band) and nanocommunications. Both TeraNets and nanocommunications will operate at THz band, which allows transmission rate up to several Tbps [12]. Jornet and Akyildiz [10] proposed the use of 100 fs-long pulses transmission by following an asymmetric On-Off Keying modulation spread in time (TS-OOK). In TS-OOK, binary 1 represents as a pulse transmission and binary 0 is silence. Pulse duration is smaller than pulse period and time between consecutive bits is fixed.

In this paper we propose simple and energy efficient image compression (SEIC) for pulse-based communication systems at THz band. The proposed method can be used in micro and macro scale. SEIC compression is based on discrete wavelet transform (DWT) transformation followed by low weight code.

Compressing an image inevitably consumes energy, hence it is important to compare the energy to transmit an uncompressed image and the energy to compress it and to send the compressed file. As it will be shown later in the article, the energy in uncompressed case is much higher than in compressed case, hence it is better to compress it before transmission.

The simulation results show that the proposed method obtain energy efficiency of more than 88 % and outperforms JPEG, JPEG 2000, GIF and PNG in terms of energy efficiency and robustness against transmission error.

Therefore, our main contributions are:

- We propose an image compression based on DWT transform and NME code, which is simple, energy-efficient and takes into account robustness.
- We compare our proposed method with several existing well known image compression methods such as JPEG, JPEG 200, GIF and PNG.
- We prove that our compression method is useful in WMSN and WMNSN.
- We show that a nano-node is able to perform perpetual image transmission according to state of the art in nano-transceiver and nano-battery.

II. Related work

Since a node in WSNs has limitation in energy capacity, both energy for computation and communication should be minimized. Simple data compression method is necessary to reduce the energy consumption in computation process. In classical WSN, image compression is required to reduce the number of transmission due to the limited bandwidth and limited-battery capacity in sensor devices [2]. Image compression can be classified as lossless and lossy. In general, lossy compression yields higher compression ratio than lossless [13]. Lossless image compression such as PNG and GIF takes the advantages of non-uniform probability distribution for a variable-length codewords. GIF uses Lempel-Ziv-Welch (LZW) code to compress image, while PNG uses deflate code, which is a variant of Lempel-Ziv.

Joint Picture Expert Group (JPEG) and JPEG 2000 are the most popular lossy image compression. JPEG is based on discrete cosine transform (DCT) transform, while JPEG 2000 on discrete wavelet transform (DWT). The results given in [14] show that DWT outperforms DCT in terms of image quality, execution time and transmission robustness, while DCT outperform DWT only in memory usage. Alternatively, memory usage in DWT can be reduced by using block processing like in JPEG [15].

Recently, there are many energy efficient codes for nanonetworks. In [16], the authors investigate the energy efficient code for TS-OOK modulation by taking into account the energy consumption at the receiver. In [17], the authors compare the performance of several low weight codes for nanonetworks in terms of energy efficiency, bandwidth expansion, channel capacity, interference reduction and transmission robustness against error.

Our new method is based on DWT transform followed by a low weight code. In image transformation, SEIC uses only the coarse coefficients, i.e. only 1 sub-band from the 4 sub-bands in original DWT. The use of a fixed codeword size in low weight code simplifies the symbol detection in decompression process compared to the variable-length codeword in DCT and DWT.

III. Background

A. Terahertz propagation model

In terahertz band, the electromagnetic propagation is affected by molecular absorption and molecular noise. The path-loss in terahertz band is mainly characterized by the spreading loss and the molecular absorption loss [18]. The spreading loss is the attenuation when electromagnetic wave propagates through the medium, while absorption loss is the attenuation due to absorbed wave's energy by molecules along the transmission path, which converts part of wave energy into internal kinetic energy at the molecule level. The molecular absorption loss can be computed as:

$$H_c(f,d) = H_{abs}\, H_{spread} \tag{1}$$

$$H_{abs}(f,d) = \exp\left(\alpha(f)\, d\right) \tag{2}$$

$$H_{spread}(f,d) = \left(\frac{4\pi f d}{c}\right)^2 \tag{3}$$

where f is the operating frequency, c is the speed of light in vacuum, d is the transmission distance and α is the molecular absorption coefficient, which depends on the molecular composition in the channel along the transmission path. The power of received pulse at a distance d from its transmitter P can be computed as:

$$P(d) = \int_B S_X(f)|H_c(f,d)|^2|H_r(f)|^2 df \tag{4}$$

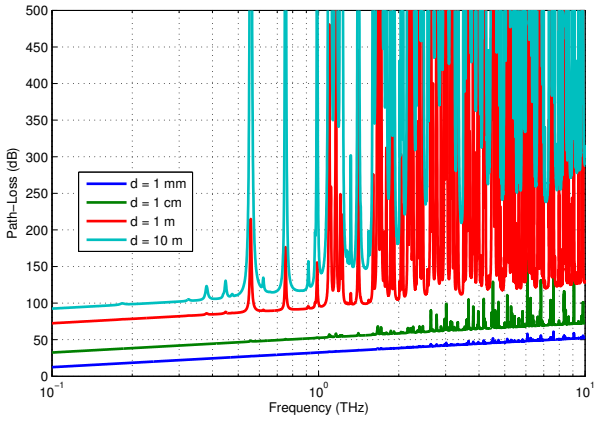

Fig. 1. Total path-loss in terahertz band using the HITRAN molecular composition database.

where B is the channel bandwidth, S_X is the power spectral density of the transmitted pulse, H_c is the channel frequency response given by (1) and H_r is the receiver's impulse response. For simplicity, we consider using match-filter receiver architecture.

In this case, the total molecular absorption noise consist of the background atmospheric noise and the self-induced noise as follows.

$$S_{N_i}(f,d) = S_{N_B}(f) + S_{N_i^X}(f,d) \tag{5}$$

$$S_{N_B}(f,d) = \lim_{d\to\infty} k_B T_0 \left(1 - |H_{abs}(f,d)|^2\right) |H_{ant}^R(f)|^2 \tag{6}$$

$$\begin{aligned} S_{N_i^X}(f,d) &= S_{X_i}(f) \left(1 - |H_{abs}(f,d)|^2\right) |H_{ant}^T(f)|^2 \\ &\quad |H_{spread}(f,d)|^2 |H_{ant}^R(f)|^2 \end{aligned} \tag{7}$$

where k_B is the Boltzmann constant, T_0 is the room temperature, H_{ant}^R and H_{ant}^R are the antenna frequency response at receiver and transmitter for an antenna that satisfies $|H_{ant}^T H_{ant}^R| = \lambda_0^2/4\pi$, where $\lambda_0 = c/f_0$ and f_0 is the center frequency of the pulse (around 1.6 THz). Therefore, the total molecular absorption noise power at the receiver N_i when symbol i is transmitted is given by

$$N_i(d) = \int_B S_{N_i}(f,d) |H_r(f)|^2 df \tag{8}$$

The probability density function of channel output Y for transmission bit $X = i$ is as follows:

$$f_Y(Y|X = x_i) = \frac{1}{\sqrt{2\pi N_i}} e^{-\frac{(y-a_i)^2}{2N_i}} \tag{9}$$

where a_i is the amplitude of received signal, which can be obtained from (4). The propagation effects at terahertz band (high attenuation and molecular noise) result in many bits received in error, especially for large transmission distance. The bit error rate (BER) is defined as the ratio between the number of bit errors and the number of transmitted bits. The BER can be computed as follows:

$$P_e = P(e|X=0)P(X=0) + P(e|X=1)P(X=1) \tag{10}$$

where $P(e|X=i)$ is the probability of bit error when bit i is transmitted and $P(X=i) = P_i$ is the probability to transmit bit i. Jornet et al. [19] consider an asymmetric terahertz channel with the following error transition probabilities:

$$P(e|X=0) = P(Y=1|X=0) = 1 - \int_A^B f_Y(Y|X=0)dy \tag{11}$$

$$P(e|X=1) = P(Y=0|X=1) = \int_A^B f_Y(Y|X=1)dy \tag{12}$$

where A and B are two threshold values. These values can be computed from the intersection of two Gaussian distributions $\mathcal{N}(0, N_0)$ and $\mathcal{N}(a_1, N_1)$ as follows:

$$A, B = \frac{a_1 N_0}{N_0 - N_1} \pm \frac{\sqrt{2N_0N_1^2 log(N_1/N_0) - 2N_0^2 N_1 log(N_1/N_0) + a_1^2 N_0 N_1}}{N_0 - N_1} \tag{13}$$

where a_1 is the amplitude of the received pulse.

B. TS-OOK modulation

Jornet et al. [10] proposed the Time-Spread On-Off Keying (TS-OOK) modulation based on very short pulses (one hundred femtosecond-long per Gaussian pulse). For the time being, the only feasible way for electromagnetic nanocommunications is pulse-base modulation. Such pulses have been used in terahertz imaging and biological spectroscopy [20]. During the transmission process, binary 1 is considered as a pulse transmission, while binary 0 as silence (no energy required). The time T_s between two consecutive symbols is much longer than the pulse duration T_p, i.e. $\beta = T_s/T_p \gg 1$. Larger TS-OOK pulse energy, larger the transmission distance can be obtained. Using eq. (10), the BER for various pulse energy is shown in Fig. 2. In order to meet the BER requirement for image transmission BER = 10^{-3}, TS-OOK modulation with pulse energy 1 aJ supports for transmission distance up to several millimeters, while 1 pJ up to several meters.

We motivates the use of TS-OOK pulse energy 1 fJ, since such compact the terahertz signal generator and detector have been reported in [21], [22].

C. NME code

In TS-OOK modulation, the transmission energy can be reduced by using low weight codes [17]. NME [23] is one such code we have proposed in the past. It obtains energy efficiency by reducing the number of bits 1 in binary sequence. This method uses simple mapping from input symbol to its corresponding codeword (coding table). An example is given in Table I. The most frequent symbols are mapped to codewords with fewer bits 1. In coding table, input symbols are sorted in decreasing order of their frequency, while codewords

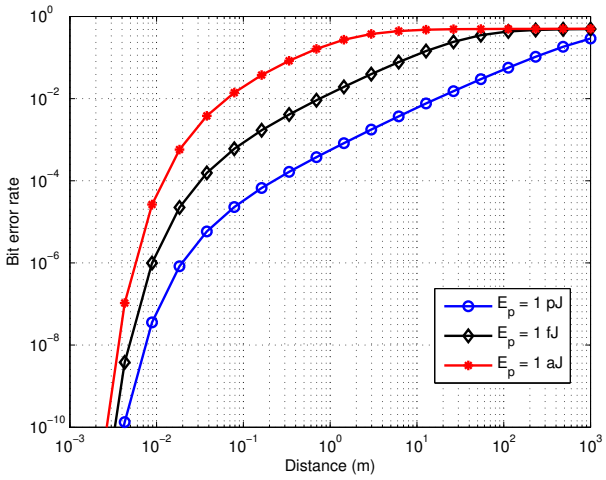

Fig. 2. BER in terahertz band with various pulse energy.

TABLE I
THE EXAMPLE MAPPING TABLE FOR NME CODE.

Input symbol	Symbol frequency	NME
111	80	000
110	70	010
101	60	001
100	50	100
011	40	101
010	30	011
001	20	110
000	10	111

are sorted in increasing number of their weight (the number of bits 1 in the codeword). The codewords have the same size (length) as input symbols bits. For codewords with the same weight, the sorting allows to reduce the number of sequential bits 1, which is a useful feature in terahertz band communications.

D. Discrete wavelet transform (DWT)

Wavelet transform has a high energy compaction which makes it a very suitable candidate for image compression. It also has other properties such as, multi-resolution and progressive reconstruction that provides wavelet a powerful tool for image and video compression [24].

Wavelet-based image compression uses sub-band coding which presents the different frequency components within an image. Sub-band coding consists of a sequence of filtering and sub-sampling processes. The wavelet decomposition for image x is shown in Fig. 3. First, the input sequence x with size NxN is filtered row by row by two filters (a low pass filter h_0 and a high pass filter h_1) then sub-sampled by factor 2, which results in two outputs of length N/2 in each filter. Next, these coefficients are filtered and sub-sampled column by column with the same process as previous (and the same filters). As a result, the output y consists of four DWT coefficients (LL, LH, HL and HH) each of size (N/2) x (N/2). The LL coefficient is called approximation coefficient, while LH, HL

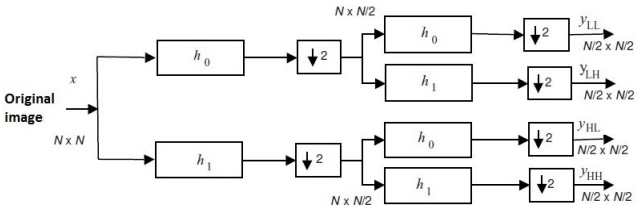

Fig. 3. Computation of a one level DWT decomposition.

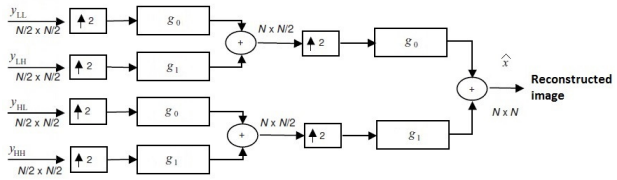

Fig. 4. Computation of a one level DWT reconstruction.

and HH are detail coefficients. The approximation coefficients result in coarse information, which contains the significant information (y_{LL}). The image compression process discards the insignificant information and maintains the significant information.

In the synthesis or reconstruction stage, the procedures are repeated in reverse direction using another set of low pass and high pass filters (a low pass filter g_0 and a high pass filter g_1). The reconstructed image has the same size as the original, and the result is close to the original image (but not the same) due to filtering effects. The reconstruction process is shown in Fig. 4.

In DWT transform, image is transformed into transform coefficients with the same size of image. Multi-level decomposition can be performed (level $i+1$) using sub-band LL_i to produce LL_{i+1}, HL_{i+1}, LH_{i+1} and HH_{i+1} bands, each with size N/(2i) x N/(2i). The process of multi-level decomposition is illustrated in Fig. 5.

IV. SIMPLE AND ENERGY EFFICIENT IMAGE COMPRESSION (SEIC)

At the sender, SEIC consists of three steps:

- Perform the first decomposition of DWT (and only this).
- Quantize the coefficients and convert them to binary stream.
- Reduce the number of bit 1 in binary stream by a low-weight code.

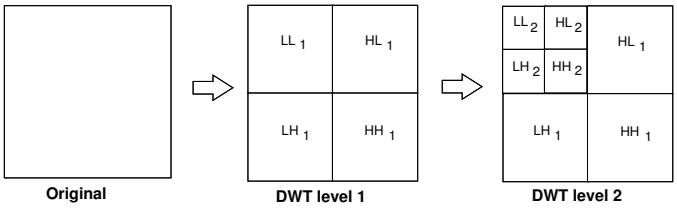

Fig. 5. Multi-level DWT transform.

These steps are shown in Fig. 6 and detailed in the following algorithm:

1) The image x is filtered row by row using low pass filter h_0 and down sampled by factor 2, then filtered column by column using filter h_1 and down sampled by factor 2. The output is y with a size of 1/4 of the input x.
2) Next, the output of transformation y is quantized by uniform scalar quantizer to fit into n bits pulse code modulation (PCM) or n bit NME code.
3) NME performs simple mapping from input symbol to a codeword, which produces binary stream for transmission.

At receiver, the reconstruction process is performed in reverse direction, i.e., NME decoding [23], de-quantization and DWT inverse transform.

The first step in SEIC algorithm is related to the obtained energy efficiency. As already stated, SEIC uses only one decomposition level. Instead, if several levels are used, the larger the level i, the larger the compression ratio which can be obtained. For example, transmitting only LL_1 yields compression ratio 4:1 and LL_2 yields 16:1 as shown in Fig. 5. Therefore, minimum energy efficiency can be estimated for each level. For example, the minimum energy efficiency using level 1 decomposition is 75 % (this value is obtained from the discard of 75 % coefficients from data input), the minimum energy efficiency for level 2 is 93 % and for level 3 is 98 %.

Our method uses only the approximation coefficient and discards the detail coefficients of DWT. SEIC is both simple and energy efficient. It is simple because:

- In a wireless node-device, the compression is performed by an electrical circuit. Compared to other DWT-based image compression methods, such as JPEG 2000, SEIC uses only 25 % of the circuit in DWT transforms. The circuit size is smaller than original DWT (i.e., use only 1 sub-band from the 4 sub-bands), which is preferable for a nano-device.
- Required memory is smaller than original DWT, due to fewer circuit/electrical components. It reduces the amount of required memory by approximately 75 % compared to JPEG 2000.
- Compared to DWT, there is no negative coefficient (negative coefficients appear only in detail coefficients), i.e. there is no additional memory to save negative sign for each of the coefficients.

It is energy efficient because:

- Due to fewer circuit/electrical in DWT components, the computation energy is smaller by approximately 75 % than original DWT.
- Output data size is reduced by 75 % from the input size in each decomposition level, i.e. each decomposition level reduces the number of coefficients by 75 % of data input. As shown in Fig. 5, the input has data size N x N, then the approximation coefficient at level i has data size N/(2i) x N/(2i). The larger the decomposition level, the larger the energy efficiency (compression ratio) which can be obtained, but the lower the reconstructed image quality.

The use of fixed codeword size in NME decoding makes symbol detection simpler, compared to variable codeword size as used in JPEG and JPEG 2000. In many cases, a 1-bit error in variable codeword size causes symbol error detection for the next symbols (error bits make impossible the reconstruction process).

V. Performance analysis

The goal of this section is to confirm the theory, i.e. computation consumes much less energy than transmission, as given in Introduction, through simulation.

In the following, we numerically investigate the performance of SEIC in terms of visual quality, energy efficiency, perpetual operation and robustness against transmission error, and compare it with several well-known compression standards (which do not use NME). In order to make our simulation more realistic, we use the following parameters: pulse width $T_p = 1\,\text{ps}$ (the first derivation of a 100 fs-long pulse results in a 1 ps-long pulse, to prevent DC component in Gaussian pulse [25]), pulse power $P = 1\,\text{mW}$ [21], so pulse energy $E_p = P\,T_s = 1\,\text{fJ}$. In wavelet transform, we use wavelet biorthogonal4.4 and quantization 8. For simulation we use MATLAB. For diversity, in the simulation we use 4 images with resolution 128x128 pixels, with different characteristics, as follows:

- Cancer cell image (`cancer128.bmp`) to represent an image with micro scale content (a cell).
- Lena image (`lena128.bmp`) to represent images with high correlation between adjacent pixels.
- Barbara image (`barbara128.bmp`) to represent images with moderate correlation between adjacent pixels.
- Baboon image (`baboon128.bmp`) to represent images with low correlation between adjacent pixels.

A. Image quality

To measure the visual quality of reconstructed images we used two classical metrics: structural similarity (SSIM) and peak signal to noise ratio (PSNR). SSIM provides results more similar to human visual perception than PSNR [26]. For both of them, the larger the value the closer the received image to the transmitted one. SSIM and PSNR for all images are shown in Table II. GIF and PNG have mean SSIM 1 and PSNR ∞ dB, which means perfect reconstruction. For lossy compression, JPEG 2000 has the largest PSNR and SEIC has the lowest PSNR for all images. As shown in Fig. 7, the SEIC image is not perfect, but is sufficiently good. This is the price to pay in order to have a simple and energy efficient compression.

B. Energy efficiency

In order to investigate the effectiveness of our compression method from energy point of view, we compare the energy in both cases, i.e. the energy to transmit the uncoded image to the energy to compress it and transmit the compressed image:

$$E_{\text{cons}}^{\text{Uncoded}} = E_{tx}^{\text{Uncoded}} \tag{14}$$

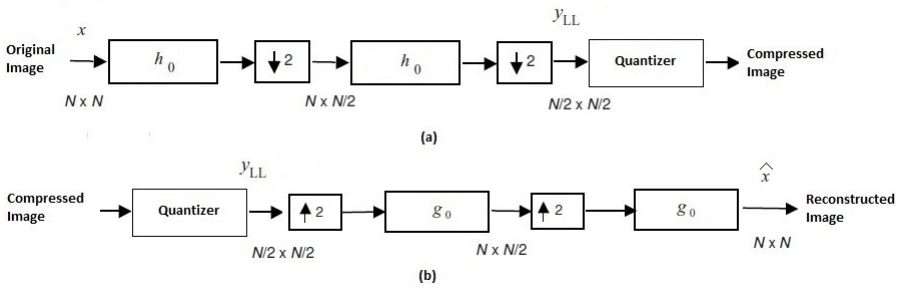

Fig. 6. Proposed method: (a) SEIC encoder, (b) SEIC decoder

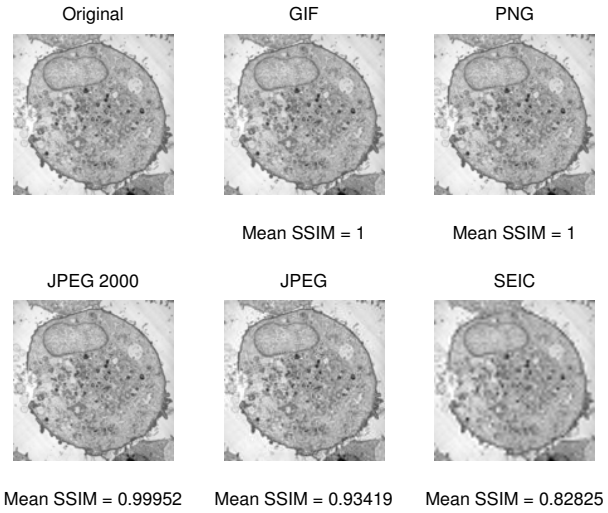

Fig. 7. Visual result of compressed Cancer image for various methods.

$$E_{\text{cons}}^{\text{Coded}} = E_{\text{comp}} + E_{\text{tx}}^{\text{Coded}} \tag{15}$$

where E_{cons} is the energy consumption, E_{tx} the transmission energy, and E_{comp} the compression energy. We present the energy on the transmitter, but similar formulas apply for receiver too.

Transmission energy. In TS-OOK modulation, the transmission energy can obtained from the number of transmitted bits 1 and pulse energy:

$$E_{\text{tx}}^{\text{Uncoded}} = N_1^{\text{Uncoded}}\, E_p \tag{16}$$

$$E_{\text{tx}}^{\text{Coded}} = N_1^{\text{Coded}}\, E_p \tag{17}$$

where E_p is the pulse energy (1 fJ) and N_1 the number of bits 1. Table II presents the transmission energy for all used methods using these formulas. Column Energy consumption on transmitter shows that the energy varies between approximately 7 000 and 76 000 fJ.

Computation energy for coded. For image with resolution 256x256 pixels, JPEG compression executes 10 million instructions on an 8-bit micro-controller. The computation energy can be reduced by factor 100 using JPEG dedicated hardware [27]. As mentioned before, the computation in a nano-device consumes 0.1 aJ [11] per instruction. So, JPEG hardware compression consumes 100 fJ. Therefore, for an image of resolution 128x128 pixels, as in our case, JPEG compression consumes $E_{\text{comp}} = 100$ fJ /4 = 25 fJ. Note that DWT transform consumes less energy than DCT [14].

The previous two paragraphs show that the compression process consumes less energy than transmission (25 fJ vs 7 000–76 000 fJ). Thus, simulation results confirm theory, as given in the Introduction.

Energy efficiency. Energy efficiency denotes the ability of code to reduce the energy consumption at transmitter side:

$$\xi = \frac{E_{\text{tx}}^{\text{Uncoded}} - \left(E_{\text{tx}}^{\text{Coded}} + E_{\text{tx}}^{\text{Comp}}\right)}{E_{\text{tx}}^{\text{Uncoded}}}\, 100\% \tag{18}$$

The energy efficiency for all images in various methods is shown in Table II, where energy for compression has been discarded since it is negligible. The results show that NME code increases the energy efficiency of DWT with only the approximation coefficients. Our proposed method (SEIC) yields more than 85 % energy efficiency.

To conclude, the energy consumption for compression is negligible compared to the energy for transmission. Therefore, it is useful to compress the image before transmitting it. Otherwise said, the energy lost by compressing an image is much lower than the energy gained by sending a compressed image.

C. Perpetual operation

The size of an individual nano-device is in the order of a few cubic micrometers [10]. In advanced health monitoring system, nano-devices can be used to detect infectious agents, such as virus and harmful bacteria [28], and sick cells. For example, cancer cells detected [29] at early stage are easier to cure. We believe that this method will revolutionize the way to cure these diseases. A nano-camera captures cell images, then transmits them to the end system for the physician diagnostic. In our application, nano-camera has 128x128 pixels resolution, so if the pixel size is 1 nm, then the size of nano-camera is around 128x128 nm^2, which still fulfills the size requirement for nano-component.

Recently, novel energy harvesting mechanisms have been proposed allowing perpetual (infinite life time) nanonetworks.

TABLE II
ENERGY EFFICIENCY FOR ALL USED METHODS (DWT APPROX MEANS DWT WITH ONLY APPROXIMATION COEFFICIENTS).

Image	Method	Energy cons. (fJ) Transmitter	Receiver	Energy eff. (%)	PSNR (dB)	SSIM
Cancer	BMP	76 223	139 696	–	–	–
Cancer	GIF	64 339	153 024	15.6	∞	1
Cancer	PNG	51 080	99 584	33.0	∞	1
Cancer	JPEG 2000	47 895	96 520	37.2	62.0	0.99
Cancer	JPEG	17 852	36 024	76.6	38.1	0.93
Cancer	DWT approx	16 229	36 992	78.7	33.1	0.83
Cancer	SEIC	7 198	36 992	90.6	33.1	0.83
Lena	BMP	65 594	139 696	–	–	–
Lena	GIF	57 797	146 640	11.9	∞	1
Lena	PNG	42 842	84 752	34.7	∞	1
Lena	JPEG 2000	37 267	75 344	45.5	60.8	0.99
Lena	JPEG	14 781	29 256	78.3	40.4	0.95
Lena	DWT approx	13 581	36 992	79.3	35.1	0.90
Lena	SEIC	7 765	36 992	88.2	35.1	0.90
Barbara	BMP	66 303	139 696	–	–	–
Barbara	GIF	59 109	149 936	10.9	∞	1
Barbara	PNG	42 196	83 280	36.4	∞	1
Barbara	JPEG 2000	36 110	72 472	42.9	60.9	0.99
Barbara	JPEG	14 410	28 552	77.2	42.4	0.97
Barbara	DWT approx	13 301	36 992	79.9	37.2	0.94
Barbara	SEIC	7 742	36 992	88.3	37.2	0.94
Baboon	BMP	69 411	139 696	–	–	–
Baboon	GIF	61 582	155 152	11.3	∞	1
Baboon	PNG	47 778	95 104	31.2	∞	1
Baboon	JPEG 2000	44 939	90 680	35.5	62.0	0.99
Baboon	JPEG	15 530	31 784	77.6	39.1	0.93
Baboon	DWT approx	14 076	36 992	79.7	35.3	0.84
Baboon	SEIC	7 082	36 992	89.8	35.3	0.84

One such mechanism is described in [9]. The vibrational energy is harvested by exploiting the piezoelectric effect of zinc oxide (ZnO) nanowires. The nano-battery capacity is approximately 200 pJ when the 9 nF nano-capacitor is charged at 0.42 V generator voltage and the number of vibration cycles is 500 cycles. For a vibrator of 2 Hz, such as in fan, the time needed to fully charge the nano-battery is 250 seconds.

The energy harvesting rate $E_{\rm hr}$ can be obtained from the nano-battery capacity 200 pJ divided by time to fully recharge it 250 seconds, which is 800 fJ/sec. The energy to transmit the cancer cell for uncoded is $E_{\rm tx} = E_p\, N_1^{\rm Uncoded} = 76\,223$ fJ. The perpetual operation for uncoded $E_{\rm hr}/E_{\rm tx} =$ 800 fJ / 76 223 fJ $\approx$ 1 image/2 minutes. For SEIC, the energy to transmit the cancer cell is $E_{\rm tx} = E_p\, N_1^{\rm SEIC} = 7\,198$ fJ. The perpetual operation for SEIC $E_{\rm hr}/E_{\rm tx} =$ 800 fJ / 7 198 fJ $\approx$ 13 images/2 minutes.

D. Robustness against transmission error

In general, compressed data is vulnerable to transmission error. One bit error may cause error propagation in reconstruction process which destroys the received image, e.g., distorted or file unable to open. This is not the case for SEIC. In this section we present the effect of error bit for transmitted image for all methods.

Using eq. (11) and (12), the transition probabilities in terahertz band is shown in Fig. 8. It shows that terahertz band is binary asymmetric channel (BAC), since bit 0 and bit 1 have different transitional probability.

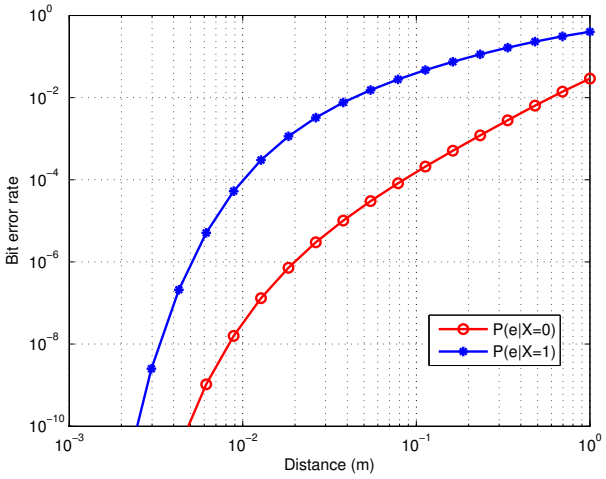

Fig. 8. Transition probabilities in terahertz band.

We investigate here the effect of error bits in the reconstruction (decompression) process at receiver. Due to limited computation in nano-devices, hard decision method is utilized in nano-receiver. The effect of error bits in reconstruction process of each compression method are different. Using the same noise at the same distance, the SSIM of various methods is shown in Fig. 9. The visual quality of reconstructed image for all methods is shown in Fig. 10. In uncoded transmission, error bits affect only certain pixels, which is also the same as SEIC method. In JPEG 2000 and JPEG, the error propagates, e.g., one bit error causes errors in many pixels. In GIF and PNG, the error results in an image which cannot be reconstructed (file cannot be opened). In order to obtain reliable transmission for compressed image, GIF, PNG, JPEG and JPEG 2000 require complex (powerful) error correction code, which is impractical for limited computation in nano-devices. While SEIC can use simple error correction code such as Hamming code, since error does not propagate in decompression process. As conclusion, SEIC method is more robust against transmission error.

VI. CONCLUSIONS

We presented a simple and energy efficient image compression (SEIC) for binary pulse-based wireless sensor networks at terahertz band. The method uses only the approximation coefficients of DWT transform followed by NME code. The simulation results show that our proposed method outperforms JPEG, JPEG 2000, GIF and PNG in several metrics: energy efficiency, perpetual operation in nanocommunications and robustness against transmission error. The trade-off is a lower image quality at receiver.

In future work we will include the computational energy to have a complete knowledge in energy consumption and perform fair comparison between image compression methods.

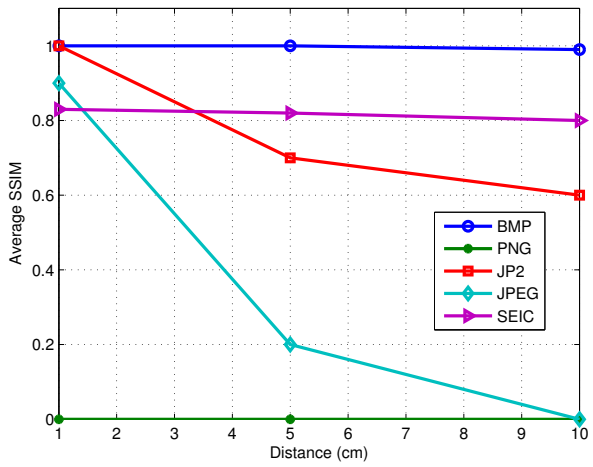

Fig. 9. The average SSIM of *received* compressed Cancer image for various methods.

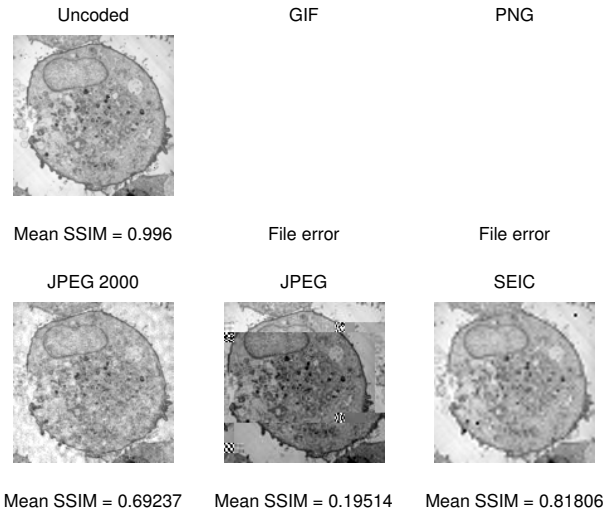

Fig. 10. Visual result of *received* compressed Cancer image for various methods.

REFERENCES

[1] I. F. Akyildiz, T. Melodia, and K. R. Chowdhury, "A survey on wireless multimedia sensor networks," *Computer Networks*, vol. 51, pp. 921–960, Mar. 2007.

[2] I. F. Akyildiz and M. C. Vuran, *Wireless Sensor Networks*. John Wiley & Sons Ltd., 2010.

[3] J. M. Jornet and I. F. Akyildiz, "The internet of multimedia nano-things," *Nano Communication Networks*, vol. 3, no. 4, pp. 242–251, Dec. 2012.

[4] G. Pottie and W. Kaiser, "Wireless integrated network sensors," *Communications of the ACM*, vol. 43, no. 5, pp. 51–58, May 2000.

[5] M. Belleville and C. Condemine, *Energy Autonomous Micro and Nano Systems*. Willey-ISTE, 2012.

[6] H. Karl and A. Wilig, *Protocols and Architectures for Wireless Sensor Networks*. Wiley, 2007.

[7] S. Chen, W. Tang, X. Zhang, and E. Culurciello, "A 64 x 64 pixels UWB wireless temporal-difference digital image sensor," *IEEE Transactions on VLSI Systems*, vol. 20, no. 12, pp. 2232–2240, Dec. 2012.

[8] M. C. Lemme, "Current status of graphene transistors," *Solid State Phenomena*, vol. 156-158, pp. 499–509, Nov. 2009.

[9] J. M. Jornet and I. F. Akyildiz, "A joint energy harvesting and communication analysis for perpetual wireless nanosensor networks in the terahertz band," *IEEE Transactions on Nanotechnology*, vol. 11, no. 3, pp. 570–580, May 2012.

[10] ——, "Femtosecond-long pulse-based modulation for terahertz band communication in nanonetworks," *IEEE Transactions on Communications*, vol. 62, no. 5, pp. 1742–1754, May 2014.

[11] N. Akkari, J. M. Jornet, P. Wand, E. Fadel, L. Elrefaie, M. G. A. Malik, S. Almasri, and I. F. Akyildiz, "Joint physical and link layer error control analysis for nanonetworks in the terahertz band," *Wireless Networks*, pp. 1–13, Aug. 2015.

[12] J. M. Jornet and I. F. Akyildiz, "Channel modeling and capacity analysis for electromagnetic wireless nanonetworks in the terahertz band," *IEEE Transactions on Wireless Communications*, vol. 10, no. 10, pp. 3211–3221, Oct. 2011.

[13] J.-N. Hwang, *Multimedia Networking: from theory to practice*. Cambridge university press, 2009.

[14] O. Ghorbel, W. Ayedi, M. W. Jmal, and M. Abid, "DCT & DWT images compression algorithms in wireless sensor networks: comparative study and performance analysis," *International Journal on Wireless & Mobile Networks*, vol. 4, no. 6, pp. 45–59, Dec. 2012.

[15] M. Angelopoulou, K. Masselos, P. Cheung, and Y. Andreopoulous, "A comparison of 2-d discrete wavelet transform computation schedules on FPGAs," in *IEEE Field Programmable Technology (FTP)*, Bangkok, Thailand, Dec. 2006, pp. 181–188.

[16] L. Huang, W. Wang, and S. Shen, "Energy-efficient coding for electromagnetic nanonetworks in the terahertz band," *Ad Hoc Networks*, vol. 40, pp. 15–25, Jan. 2016.

[17] M. A. Zainuddin, E. Dedu, and J. Bourgeois, "Low-weight code comparison for electromagnetic wireless nanocommunications," *IEEE Internet of Things*, vol. 3, pp. 38–48, Feb. 2016.

[18] J. M. Jornet and I. F. Akyildiz, "Information capacity of pulse-based wireless nanosensor networks," in *IEEE Communications Society Conference on Sensor, Mesh and Ad Hoc Communications and Networks (SECON)*, ser. 8. Salt Lake City, Utah, USA: IEEE, Jun. 2011, pp. 80–88.

[19] J. M. Jornet, "Low-weight error-prevention codes for electromagnetic nanoneworks in the terahertz band," *Nano Communications Networks*, vol. 5, no. 1-2, pp. 35–44, May 2014.

[20] D. Woolard, P. Zhao, C. Rutherglen, Z. Yu, P. Burke, S. Brueck, and A. Stintz, "Nanoscale imaging technology for THz-frequency transmission microscopy," *International Journal of High Speed Electronics and Systems*, vol. 18, no. 1, pp. 205–222, Mar. 2008.

[21] L. Vicarelli, M. S. Vitiello, D. Coquillat, A. Lombardo, A. C. Ferrari, W. Knap, M. Polini, V. Pellegrini, and A. Tredicucci, "Graphene field-effect transistors as room-temperature terahertz detectors," *Nature Materials*, vol. 11, pp. 865–871, Oct. 2012.

[22] W. Knap, F. Teppe, N. Dyakonova, D. Coquillat, and J. Lusakowski, "Plasma wave oscillations in nanometer field effect transistors for terahertz detection and emission," *Journal of Physics: Condensed Matter*, vol. 20, no. 38, p. 384205, Aug. 2008.

[23] M. A. Zainuddin, E. Dedu, and J. Bourgeois, "Nanonetwork minimum energy coding," in *IEEE International Conference on Ubiquitous Intelligence and Computing (UIC)*, ser. 11, Bali, Indonesia, Dec. 2014, pp. 96–103.

[24] K. S. Thyagarajan, *Still image and video compression with Matlab*. John Wiley & Sons, Inc., 2011.

[25] M. A. Zainuddin, E. Dedu, and J. Bourgeois, "The effects of nanosensors movements on nanocommunications," in *The 2nd ACM Nanocom*, Boston, Massachusetts, USA, Sep. 2015, pp. 1–6.

[26] Z. Wang, A. Bovik, H. Sheikh, and E. Simoncelli, "Image quality assessment: from error visibility to structural similarity," *IEEE Transaction on Image Processing*, vol. 13, no. 4, pp. 600–612, Apr. 2004.

[27] V. G. Oklobdzija, *Digital Design and Fabrication*. CRC Press, Taylor and Francis Group, 2007.

[28] P. Tallury, A. Malhotra, L. M. Byrne, and S. Santra, "Nanobioimaging and sensing of infectious diseases," *Advanced Drug Delivery Reviews*, vol. 62, no. 4, pp. 424–437, Mar. 2010.

[29] I. E. Tothill, "Biosensors for cancer markers diagnosis," *Seminars in Cell & Developmental Biology*, vol. 20, no. 1, pp. 55–62, 2009.